

# Analysis of mechanical properties of single wall carbon nanotubes fixed at a tip apex by atomic force microscopy

D Dietzel<sup>1</sup>, Marc Faucher<sup>2</sup>, Antonio Iaia<sup>3</sup>, J P Aimé<sup>1</sup>,  
S Marsaudon<sup>1</sup>, A M Bonnot<sup>3</sup>, V Bouchiat<sup>4</sup> and G Couturier<sup>1</sup>

<sup>1</sup> CPMOH, Université Bordeaux 1, 351, cours de la Liberation F-33405 Talence, France

<sup>2</sup> LETI CEA, 17 Avenue des Martyrs, F-38042 Grenoble, France

<sup>3</sup> LEPES CNRS, 166X F-38042 Grenoble Cedex 9, France

<sup>4</sup> CRTBT CNRS, 166X F-38042 Grenoble Cedex 9, France

E-mail: jp.aime@cpmoh.u-bordeaux1.fr

Received 24 November 2004, in final form 16 December 2004

Published 14 January 2005

Online at [stacks.iop.org/Nano/16/S73](http://stacks.iop.org/Nano/16/S73)

## Abstract

An investigation of the mechanical properties of single wall carbon nanotubes (SWNT) fixed at a tip apex was performed using a frequency modulation-atomic force microscope (FM-AFM). The FM-AFM method allows the measurement of conservative and non-conservative forces separately and unambiguously. The FM-AFM analysis provides information that aids the understanding of the effects of the interaction between the free SWNT end and the surface: the resonant frequency shifts provide information on the effective SWNT spring constant, while the damping signal gives information on the type of contact between the tube and the surface. The variation of the damping signal as a function of the tip surface distance shows that the additional energy loss produced by the interaction between the tube and the surface is mostly due to an adhesion hysteresis. As a result, the increase of the damping signal is correlated to the existence of intermittent contact situations. The whole variations show how the contact between the free SWNT end and the surface modifies the elastic response of the tube.

(Some figures in this article are in colour only in the electronic version)

## 1. Introduction

Carbon nanotubes (CNTs) have diameters ranging from 1 to 100 nm and lengths that can reach values up to several mm, thus CNTs possess the unique combination of nanometre and large, macroscopic, sizes [1]. Additionally, they are characterized by high stiffness, high strength and a broad range of electronic properties.

Thus, the variety of their applications [2], which have been developed after the discovery of CNTs in 1991 [3], is immense: e.g. high strength reinforcing elements in composites, connecting components in nanoscale electronics and AFM tips. In particular, for AFM tips, the application of nanotubes seems very promising, since these tips have

a lot of advantages in key properties of cantilever tips: in particular the chemically inert CNTs have a large aspect ratio allowing various surface structures with steep edges to be readily investigated. Also the combination of the geometrical parameters of CNTs and a high elastic modulus (of about the THz) gives the opportunity of having both high mechanical strength for the tube elongation and a flexible behaviour. Therefore, AFM tips ending in CNTs should be a good candidate for preventing wear modification of the tip apex.

Basically, two groups of CNTs can be distinguished: the first to be discovered, multiwalled carbon nanotubes (MWNT), consist of nested, concentric tubes [3, 4]. The others are the so-called single wall CNT (SWNT), which involve a single rolled-up graphite sheet. SWNTs with diameters smaller than that

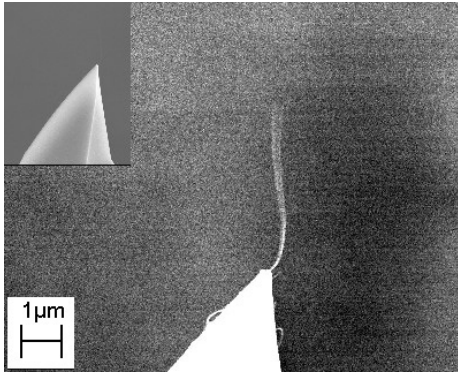


**Figure 1.** Scanning electron microscopy of a Si cantilever tip with a SWNT self-bound to the apex using the hot filament assisted CVD technique. For an easier view, the contrast of the image has been enhanced.

of MWNTs are especially interesting for AFM applications requiring a very high spatial resolution.

However, attaching a CNT at the apex of a commercial Si tip drastically modifies the mechanical behaviour of the Si tip–cantilever system approaching a surface. The resonance frequency shift and the damping signal in FM-AFM should now mostly reflect the mechanical response of the CNT instead of the usual tip surface interaction [5–7].

Information about the nanotubes themselves is of primary importance; however their mechanical properties are hardly accessible by standard techniques of mechanical characterization [8]. In that context, the measurements of the resonant frequency shift and of the damping signal with a FM-AFM can provide a valuable contribution in understanding the system made of an AFM cantilever and a CNT.

In addition to the usual analysis of the evolution of the resonance frequency shift and of the damping signal as a function of the tip surface distance, the greatest difficulty to overcome is to evaluate the influence of the mechanical response of the tube as a function of the contact between the free tube end and the surface. An attempt to address this complex problem will be to consider two limiting and opposite cases: one corresponding to the tube end pinned on the surface, the second where the tube end is able to slide freely on the surface. Then, the experimental results are discussed and compared to predictions from a simple analytical development modelling the resonant frequency shift as a function of the mechanical deformation.

## 2. Experimental methodology

SWNT probes (figure 1) are fabricated using a hot filament assisted CVD technique [9] that ensures simultaneous growth and binding of SWNTs at the apex of commercial AFM tip covered by a thin cobalt catalyst layer [10]. The AFM experiments are performed with a modified Nanoscope Digital Instrument Head NII [11]. The resonance frequency of the vibrating cantilever,  $\nu_0 = 286.400$  kHz, and the quality factor,  $Q = 530$ , are extracted from the resonance curves recorded in ambient conditions. The spring constant is estimated to be  $k_c = 20$  N m<sup>-1</sup>.

For FM-AFM operation, a sinusoidal excitation locked at the resonance frequency keeps the amplitude of the cantilever

oscillation constant. The basic principle follows the FM-AFM method [12] using a PLL controller<sup>5</sup> for frequency demodulation. In this work, we focus on approach and retract curves in which the shift of the resonance frequency and the variation of the damping signal are recorded as a function of the tip surface distance. By providing sinusoidal excitation always fixed at the resonance frequency, conservative and non-conservative forces can be measured separately [13, 14]. In addition, when the oscillation amplitude is kept constant, the damping signal contains information on the additional losses of energy per period due to the interaction between the tip and the sample.

In the next two sub-sections we introduce a few mathematical expressions that are useful for the analysis of the experimental data. Following a number of previous experimental and theoretical works, equations derived from differential geometry are well adapted to describe the elastic behaviour of wires with diameters of nanometre size and in particular for CNTs [15–17]. This short introduction aims at showing the influence of the boundary conditions on the mechanical responses of the CNT. Then, a method based on the variational principle of least action [5, 14] is introduced to analyse the resonance frequency shifts as a function of the mechanical properties of the CNT.

### 2.1. Mechanical properties of CNTs squeezed between a tip and a surface

Although the Young modulus of CNTs can be as high as  $E = 10^{12}$  N m<sup>-2</sup>, when these tubes are long and thin they can become very flexible with a low bending spring constant. To simplify the discussion, we consider an undeformed straight cylinder tube. The tube is squeezed between the tip and the surface, and, when the surface is moved towards the tip, the elastic displacement is first described as a bending deformation.

The equilibrium state of a straight tube corresponds to a radius of infinite curvature. If  $R(s)$  denotes the radius of curvature at curvilinear coordinate  $s$  after an external force has been applied, the elastic bending energy is [18]:

$$E_{\text{CNT}} = \frac{1}{2}EI \int ds \left( \frac{1}{R(s)} \right)^2 \quad (1)$$

where  $I$  is the momentum of inertia of the tube section (for a tube of radius  $r$ ,  $I = \pi r^4/4$ ) and the integration is done over the contour length  $L$ . When considering a vertical displacement  $z$ , when the CNT end slides freely on the surface, the vertical displacement leads to the same lateral displacement. Then, with  $\mathbf{I}(s)$  the vector location of a point on the cylinder, the curvature of the tube is  $1/R(s) = d^2\mathbf{I}/ds^2 \sim 2z/L^2$ , so that:

$$E_{\text{CNT}} = \frac{1}{2}E \frac{\pi r^4}{4} L \frac{4z^2}{L^4}. \quad (2)$$

Equation (2) can be rewritten with an equivalent spring constant  $(1/2)k_B z^2$  and leads to the bending spring constant:

$$k_B = E\pi r^4/L^3. \quad (3)$$

<sup>5</sup> Easy PLL FM-detector and sensor controller [www.nanosurf.com](http://www.nanosurf.com)

Thus, for CNTs long and thin, the bending spring constant can be less than  $10^{-4} \text{ N m}^{-1}$ , for example with  $E = 10^{12} \text{ N m}^{-2}$ ,  $r = 2 \text{ nm}$  and  $L = 1 \mu\text{m}$ ,  $k_B = 2 \times 10^{-5} \text{ N m}^{-1}$ . Thus, the spring constant can be several orders of magnitude smaller than that of the cantilever. On the other hand, the spring constant corresponding to tube elongation is much larger than the bending spring constant. The spring constant  $k_c$  corresponding to tube elongation is:

$$k_c = E\pi r^2/L. \quad (4)$$

Considering the ratio between the two springs scales as  $k_c/k_B \sim (L/r)^2$ , with  $r = 2 \text{ nm}$  and  $L = 2 \times 10^3 \text{ nm}$ ,  $k_c$  is six orders of magnitude larger than  $k_B$ .

However, it is worth noting that only a fraction of the tube might be involved in the elastic force, so that the effective contour length one has to use in equation (3) can be smaller than the observed one (figure 1). Since the spring constant has a cubic power law dependence on the contour length, any change of the effective contour length leads to significant variations of the spring constant.

In the next sub-section, we turn to a discussion on the way one can access the mechanical response of the CNT with the FM-AFM method.

## 2.2. Relationship between the CNT mechanical responses and the resonant frequency shifts

In spite of the simple description of the tube's elasticity, the experimental set up corresponding to a tube squeezed between a tip and a surface might lead to a complex elastic response with a combination of spring constants ranging from  $10$  to  $10^{-4} \text{ N m}^{-1}$ . For further analysis, we assume that the elongation spring constants, or in general spring constants much larger than the bending one, only contribute during the unsticking of the free end of the CNT from the surface. Therefore, one expects a noticeable change in the curve of the resonant frequency shifts when the transition from intermittent contacts to permanent contacts between the tube and the surface takes place.

In addition to that, the effective force gradient varies as the intermittent contact increases over an oscillation period. Assume that the type of tube deformation remains always the same over the whole domain of intermittent contact situations, then only one effective spring constant is involved in the frequency shift. When the tube deformation is given by the distance between the tip and the surface, the relative resonance frequency shift is [18]:

$$\frac{(v - v_0)}{v_0} \approx \frac{1}{2} \frac{k_{NT}}{\pi k_c} \left( d\sqrt{1 - d^2} - \arccos(d) \right). \quad (5)$$

Equation (5) is derived using a variational principle [18], where  $d$  is a reduced coordinate [5], and is the ratio of the tip surface distance and of the oscillation amplitude.

When the free CNT end is permanently touching the surface, corresponding to  $d = -1$  in equation (5), the expression between the effective tube spring constant  $k_{NT}$  and the resonance frequency shift simplifies:

$$\Delta v = v_0 \left( \sqrt{1 + \frac{k_{NT}}{k}} - 1 \right). \quad (6)$$

The low value of the bending spring constant requires the capability of measuring the force gradient around  $10^{-4} \text{ N m}^{-1}$ . Such high sensitivity is readily obtained with a FM-AFM using a cantilever with a spring constant of  $10 \text{ N m}^{-1}$ . Then for a force gradient of  $10^{-4} \text{ N m}^{-1}$ , the relative resonance frequency shift is of only  $5 \times 10^{-6}$ . For a resonance frequency of about  $300 \text{ kHz}$ , the corresponding shift is about  $1.5 \text{ Hz}$  and can be measured with commercially available frequency demodulators [12] (see footnote 5).

When the tube permanently touches the surface, one should measure a constant resonant frequency shift, from which it is easy to calculate an effective spring constant (equation (6)). For the present experiments, the spring constant can be either related to a simple deformation or to a combination of tube deformations leading to a contribution of different spring constants. Therefore, even when a simple linear elastic behaviour is considered, the mechanical response of the squeezed tube can lead to complicated variations of the force.

In addition to conservative forces of the tip sample interaction, one has also to consider dissipative interactions that give rise to additional energy losses during each oscillation period. Dissipation manifests itself as a hysteresis of the force versus displacement curve. Dissipation mechanisms may involve electrical losses and time delays, as happens in viscoelastic materials [13], or mechanical instabilities due to adhesion [6, 14].

The discrimination between the contribution of viscous processes and mechanical instabilities to energy loss might be sometimes difficult to achieve. However, there are several features specific to each mechanism. Energy loss due to viscous effect exhibits oscillation amplitude dependence and, when soft materials are involved, an indentation depth dependence [13]. For adhesion hysteresis, without any viscous effect, an instability criterion governs the energy loss, and thus must exhibit a threshold value during the vertical displacement that depends on the CNT stiffness and the geometry of the contact. Consequently, the additional damping signal does not depend on the oscillation amplitude and on the tip surface distance.

To summarize, section 2 emphasizes the influence of the interaction between the free CNT end and the surface. The boundary conditions between the free CNT end and the surface can vary significantly from a free sliding condition to a sticking one. Then, different types of contact between the CNT and the surface will lead to different mechanical responses of the squeezed tube as a function of the vertical displacement of the surface.

An immediate consequence is that, even within this simplified framework of a linear elastic response, a more or less complex resonant frequency shift and damping signal evolution can be observed.

## 3. Experimental results and discussion

Experiments were recorded on silica and graphite in air. The approach-retract curves are classified in two categories: in the first one the vertical displacement is large, over several hundred nanometres, while the other one corresponds to small vertical displacements of a few tens of nanometres. The latter

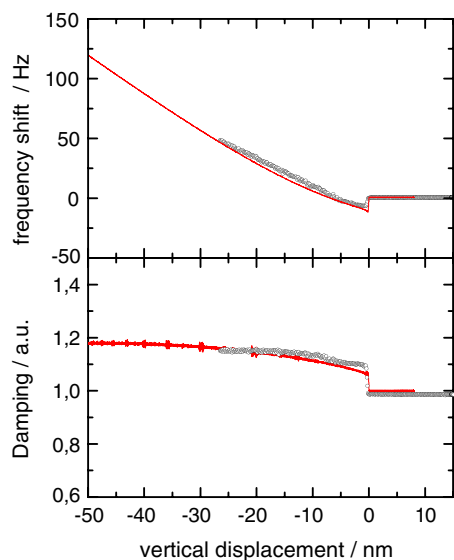


**Figure 2.** Magnification of the beginning of an approach curve showing first the decrease then the increase of the frequency shift and the corresponding change of the damping with the vertical displacement of the surface. The oscillation amplitude is  $A = 50$  nm. Comparison between a numerical simulation using a virtual AFM [11, 18] (continuous curve) and the experimental data (empty circle).

curves focus on the very beginning of the curves, for which the transition between intermittent and permanent contact situations is investigated, while the first one deals with the study of the whole behaviour of the SWNT. In particular, the effects of the transition between intermittent and permanent contact between the free tube end and the surface can be investigated.

The very beginning of the variation of the resonant frequency shifts and of the damping as a function of the vertical displacement is displayed in figure 2. The tube touches intermittently the surface over a vertical displacement of about twenty nanometres. The abrupt decrease of the resonant frequency shift occurs within a vertical displacement of the surface less than the nanometre and corresponds to a dominant attractive interaction between the tip and the surface. Then, the frequency shift begins to increase, corresponding to the point at which the tube touches intermittently the surface. As usual, the resonance frequency shift shows two monotonous variations, first a decrease corresponding to attractive interaction, then an increase corresponding to repulsive interaction. The latter varies over a large vertical displacement of the tube squeezed between the tip and the surface. The fact that repulsive regimes can be observed over a large domain of vertical displacements can be simply understood by the fact that the associated spring constant of the tube is much smaller than that of the cantilever. Note that the negative frequency shift is not always observed. The absence of negative frequency shifts means that some contacts occur between the tube and the surface, from which either the attractive interaction is too weak to be measured or the frequency shift is dominated by repulsive forces (figure 3). This is especially obvious when the intermittent contact region begins with a jump of about 100 Hz (figure 3(b)). This frequently observed behaviour might be related to a geometrical configuration, where the

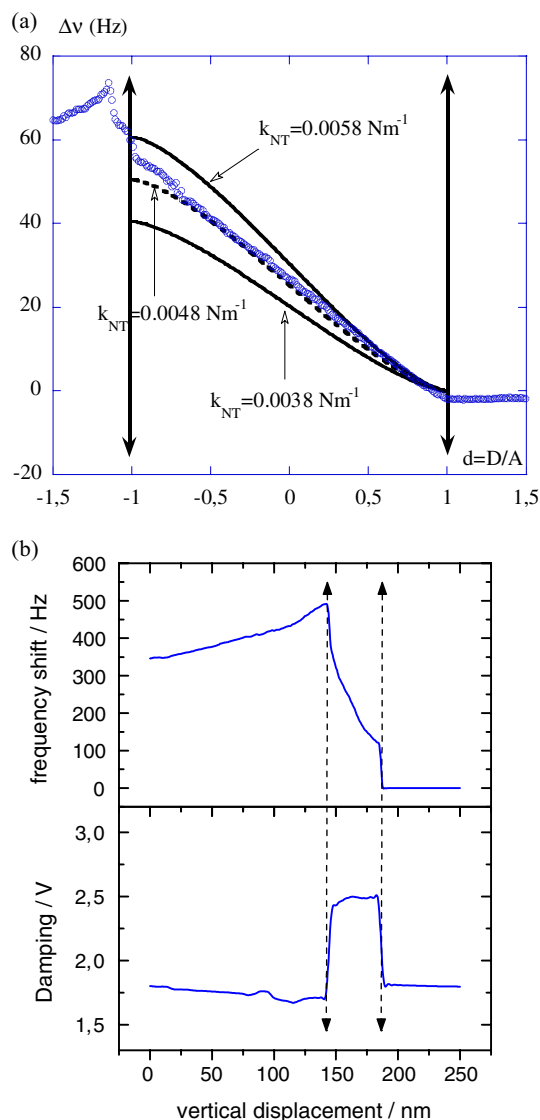


**Figure 3.** Approach curves showing variation of the frequency shift and damping with the vertical displacement of the surface. The double arrows indicate the beginning and the end of the intermittent contact situation. (a) Comparison between theoretical curves calculated with equation (5) and the experimental variation of the frequency shift in the intermittent contact situation. The dotted line corresponds to the spring constant giving the best agreement with the experimental data. (b) Approach curve with a larger domain of vertical displacement showing the smooth decrease of the resonance frequency shift in the full contact situation. Note that the maximum of the frequency shift is six times larger than the one shown-in (a).

tube is very straight relative to the sample surface. In this configuration, the comparatively smooth bending process does not start immediately, but a threshold force must be applied such that the tube starts to slide and bend.

Whatever the type of variation of the resonance frequency shift at the very beginning of the curve, for all cases, at the vertical location where the resonant frequency starts to increase, a jump of the damping signal occurs. The increase of the damping is large as it corresponds to an increase of about fifteen percent of the damping coefficient. Since the oscillation amplitude is  $A = 50$  nm, the energy loss per period when the tip does not interact with the surface is

$E_{\text{diss}} \sim kA^2/Q = 20 \times 25 \times 10^{-16}/500 = 10^{-16} \text{ J} \sim 500 \text{ eV}$  and the additional loss of energy deduced from the height of the jump is about 75 eV. As it has yet been observed with multi wall nanotubes tips [18], when CNTs are involved in the dissipation process, the main origin of the additional damping is due to adhesion hysteresis. Using a virtual AFM machine [11, 18], the result of a numerical simulation gives an excellent agreement between the magnitude of the negative frequency shift, related to attractive interaction and the height of the damping jump related to the adhesion force (figure 2). From the jump height and the energy loss evaluation, the corresponding force is about 0.2 nN.

Equation (5) predicts a dependence of the resonance frequency with the vertical location, from which a spring constant can be extracted. As an example, figure 3(a) shows a comparison between the calculated curve and the experimental data. The fit procedure gives a spring constant  $k_{\text{NT}} \sim 0.0048 \text{ N m}^{-1}$ . This value is greater than the one we may expect from the geometrical parameter of the SWNT (figure 1). This quite large spring constant suggests that the tube end is unable to freely slide. On the other hand, it is ten times smaller than those obtained with a MWNT 10  $\mu\text{m}$  long and 80 nm in diameter [18]. However, when elastic deformations are mostly connected to bending of the tube, the spring constant  $k_{\text{NT}}$  strongly depends on the geometrical parameters. Thus, the mechanical response of the tube, in turn the resonant frequency shift, can show significant variations that depend on the effective contour length involved in the whole tube deformation.

In order to have a more accurate estimation of the spring constant determination, theoretical curves corresponding to changes of 20% on the spring constant value are shown: 0.0038 and 0.0058  $\text{N m}^{-1}$ , respectively. These two theoretical curves are significantly different from the best fit and also differ markedly from the experimental data, while the one with  $k_{\text{NT}} = 0.0048 \text{ N m}^{-1}$  is fairly close to the experimental curve.

However, because we can observe a wide range of frequency shifts, see as an example, the results shown in figure 3(b), due to different types of contact between the tube and the surface, the value of the spring constant in itself cannot be totally meaningful.

In figure 3(b) a complete variation of the resonant frequency shift and damping evolution is shown. An increase of the damping coefficient is only observed when intermittent contacts between the tip and the surface take place. Thus, as shown with our numerical calculation and the experimental data (figure 2), the physical origin of the additional damping is mostly due to the hysteresis of adhesion as the result of an unsticking force when the tip completely retracts from the surface during the cycle. The unsticking force obviously is not required during the approach and thus produces the difference in force within a cycle between the approach and the retract motion.

When the surface is moved towards the sample by about 200 nm, we obtain a domain of vertical displacement for which the tube permanently touches the surface. While the intermittent contact region always shows the same behaviour, as discussed above, for the full contact situations the frequency shift remains comparatively unchanged and the damping signal exhibits an almost constant value, nearly equal to the one

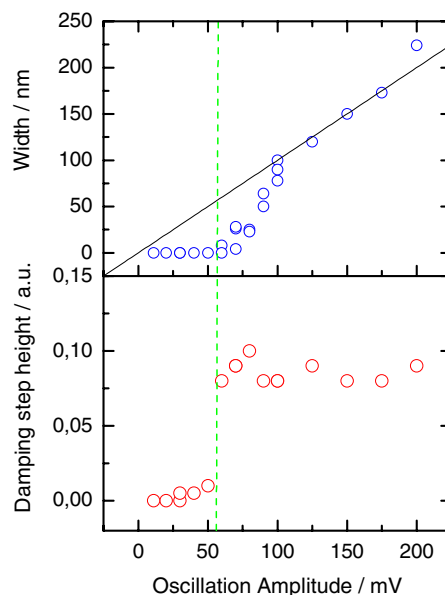


**Figure 4.** Top: variation of the width of the intermittent contact region delimited by the two arrows in figure 3(a) as a function of the oscillation amplitude  $A$ . Below a given oscillation amplitude, the width collapses to a zero value corresponding to a permanent contact over the oscillation period. Bottom: corresponding variation of the additional damping coefficient. As expected with the permanent contact situation, the additional damping goes to zero as the width of the intermittent contact situation goes to zero.

observed when the tip does not interact with the surface. Especially the constant frequency shift is interesting, as it indicates that for the full contact situation the nanotube remains pinned and the force constant can be directly calculated from equation (6). For example, a frequency shift of 300 Hz leads to a spring constant  $k = 0.042$ , thus about an order of magnitude larger than the one deduced from the fit in figure 3(a). In this case, the tube experiences a complete different contact with the surface, certainly a more efficient adhesion than in the case of figure 3(a).

To end the presentation of the experimental results, we report the variation of the size of the intermittent contact situation as a function of the oscillation amplitude (figure 4). The domain of vertical displacement over which intermittent contact situations occur must scale as twice the oscillation amplitude [18], and thus should show a linear dependence as a function of the oscillation amplitude. Such a result is approximately correct when large oscillation amplitudes are used. However, when the oscillation amplitudes are below a threshold value, the domain of vertical displacement over which intermittent contact situations occur falls to zero. Therefore, when the oscillation amplitudes become too small, as soon as the SWNT touches the surface the tube is unable to unstick over a cycle of oscillation. One reason we can put forward is that the spring constant of the SWNT is not large enough to unstick the tube from the surface. In any cases, this drastic variation of the evolution of the frequency shift as a function of the oscillation amplitude is a result of a transition from intermittent contact situations between the tube and the surface to permanent ones.

The corresponding variation of the damping signal strongly supports the above interpretation, as the additional

damping falls to a null value when the width of the intermittent domain goes to zero. This result is in complete agreement with the analysis of the physical origin of the damping. When intermittent contact situations take place, over a cycle the interaction forces are not identical during the approach and the retraction of the tip. When the surface is retracted, a force is required to unstick, thus producing an adhesion hysteresis and an additional damping coefficient. When a permanent contact occurs over the whole oscillation, the hysteresis of adhesion disappears, and in turn the additional loss of energy due to the interaction between the tip and the surface.

#### 4. Conclusion

An investigation of the SWNT mechanical properties was performed using a FM-AFM with a PLL electronic. The FM-AFM method is very sensitive and the measurement of a spring constant five orders smaller than that of a cantilever stiffness of  $20 \text{ N m}^{-1}$  can be performed. Moreover, the FM-AFM method allows the measurement of conservative and non-conservative forces separately. In particular, the damping signal contains information on the additional energy losses per period due to tip sample interaction. Then, when the resonant frequency shifts and damping signals are simultaneously recorded, a coherent picture of the SWNT mechanical response is obtained.

The SWNT is firmly stuck on the tip so that the main parameter governing the mechanical response of the tube in interaction with a surface is the contact between the free SWNT end and the surface. The variations of the damping signal indicate that additional energy losses are mostly due to adhesion hysteresis. The whole variations of damping and frequency shift show how the contact between the free SWNT end and the surface modifies the elastic response of the tube and in turn the spring constant measured by the frequency shifts. When the CNT experiences intermittent contact situations, the spring constant is rather large corresponding to a tube end pinned on the surface. An analytical model can be used providing information is known on the associated spring constant describing the elastic properties of the tube. A decrease, or disappearance, of the additional damping corresponds to a transition to a permanent contact.

A useful result is the abrupt change of the damping connected to intermittent contact situations in which hysteresis of adhesion occurs. Such a damping variation might be a way

to get accurate control of the tip surface distance, just by using a light contact of the tube.

#### Acknowledgment

The authors gratefully acknowledge the financial support provided by the Region Aquitaine.

#### References

- [1] Zhu H W, Xu C L, Wu D H, Wei B Q, Vatjai R and Ajayan P M 2002 *Science* **296** 884
- [2] Dresselhaus M S, Dresselhaus G and Avouris Ph (ed) 2001 *Carbon Nanotubes: Synthesis, Structure, Properties and Applications (Springer Topics in Applied Physics vol 80)* (Berlin: Springer)
- [3] Iijima S 1991 *Nature* **354** 56
- [4] Nguyen C V, Chao K J, Stevens R M D, Delzeit L, Cassel A, Hans J and Meyyappan M 2001 *Nanotechnology* **12** 363
- [5] Nony L, Boisgard R and Aimé J P 1999 *J. Chem. Phys.* **111** 1615  
Aimé J P, Boisgard R, Nony L and Couturier G 1999 *Phys. Rev. Lett.* **82** 3388
- [6] Dürig U 2000 *New J. Phys.* **2** 5.1
- [7] Hölscher H, Gotsmann B, Allers W, Schwarz U D, Fuchs H and Weisendanger R 2001 *Phys. Rev. B* **64** 75402
- [8] Salvetat J-P, Kulik A J, Bonard J-M, Briggs G A D, Stöckli T, Méténier K, Bonnamy S, Béguin F, Burnham N A and Forró L 1999 *Adv. Mater.* **11** 161
- [9] Marty L, Bouchiat V, Naud C, Chaumont M, Fournier T and Bonnot A M 2003 *Nano Lett.* **3** 1115
- [10] Marty L, Iaia A, Faucher M, Bouchiat V, Naud C, Chaumont M, Fournier T and Bonnot A M 2005 *Thin Solid Films* at press
- [11] Couturier G, Boisgard R, Nony L and Aimé J P 2003 *Rev. Sci. Instrum.* **74** 2726–34
- [12] Albrecht T R, Grütter P, Horne D and Rugar D 1991 *J. Appl. Phys.* **69** 668
- [13] Boisgard R, Aimé J P and Couturier G 2002 *Surf. Sci.* **511** 171  
Dubourg F, Aimé J P, Marsaudon S, Boisgard R and Leclère P 2001 *Eur. Phys. J. E* **6** 49–55
- [14] Dürig U 1999 *Surf. Interface Anal.* **27** 467
- [15] Cuenot S, Demoustier-Champagne S and Nysten B 2000 *Phys. Rev. Lett.* **85** 1690
- [16] Kis A, Kasas S, Babić B, Kulik A J, Benoît W, Briggs G A D, Schönenberger C, Catsicas S and Forró L 2002 *Phys. Rev. Lett.* **89** 248101
- [17] Landau L D and Lifshitz E M 1959 *Theory of Elasticity* (London: Pergamon)
- [18] Dietzel D, Marsaudon S, Aimé J P, Nguyen C V and Couturier G 2005 submitted